www.czasopisma.pan.pl PAN POLSKA AKADEMIA NAUK www.journals.pan.pl

ARCHIVE OF MECHANICAL ENGINEERING

DOI: 10.24425/ame.2025.154735 2025, Vol. 72, No. 2, pp. 221–247

Jaime GALLARDO-ALVARADO [1]

Similar motions, an innovative concept in kinematic redundancy resolution applied in a (3+2)-degree-of-freedom planar parallel manipulator

Received 15 February 2025, **Revised** 6 May 2025, **Accepted** 15 May 2025, **Published online** 20 May 2025

Keywords: parallel manipulator, kinematic redundancy, screw theory

This paper introduces the concept of *similar motions* to solving the kinematic redundancy problem of parallel manipulators. The method is applied to the analysis of a kinematically redundant parallel manipulator in which the redundancy is obtained with the addition of two extra prismatic joints. The kinematic analysis assumes that the conditions introduced by the additional degrees of freedom are known a priori and thus avoids the classical application of the pseudo-inverse Jacobian matrix. Kinematic redundancy is used in such a way that the two additional kinematic pairs perform motions similar to those assigned to the moving platform, an introductory concept that has not been considered in previous works. The position analysis allow for obtaining all its possible solutions while the velocity input-output equation of the parallel manipulator is obtained by resorting to screw theory and dispenses with passive joint rates thanks to the application of reciprocal line cancellation properties via the Klein form. In this way, the kinematic analysis method is computationally efficient, which is demonstrated solving numerical examples.

1. Introduction

Kinematic redundancy emerges when a robotic manipulator has more degrees of freedom than those strictly necessary to perform a given task. In the first instance, an indisputable advantage is that the end effector or moving platform of a kinematically redundant manipulator can reach the same position and orientation in multiple ways. This redundancy allows for greater flexibility in movement and the ability to avoid obstacles, optimize certain criteria related to energy consumption

✉ Jaime GALLARDO-ALVARADO, email: jaime.gallardo@itcelaya.edu.mx
[1] National Technological Institute of Mexico, Celaya, Mexico

or joint limits as well as improve accuracy and dexterity. In its early days, kinematic redundancy focused on serial manipulators [1–6], which is not surprising considering that the study of the human arm has spurred an exhaustive research area since the time of Leonardo da Vinci. The need for kinematic redundancy was quickly pointed out by NASA which was consolidated in the development of dexterous telerobots capable of simultaneously coordinating the control of mechanical arms composed of more than six joints [7]. Given the limitations of workspace and manipulability of parallel manipulators, the subject was incorporated as a relevant topic of great utility in these complex mechanisms, which has not gone of course unnoticed in academia. Wang and Gosselin [8] proposed the design of a spherical parallel manipulator and a Stewart platform, both with an additional degree of freedom in order to overcome singular configurations. Ebrahimi et al. [9] addressed the inverse position and singularity analyses of a planar parallel manipulator provided with three additional degrees of freedom, and demonstrated by comparing the workspace of the kinematically redundant parallel manipulator with that of its non-redundant counterpart the superiority of the former. Jiang et al. [10] performed force optimization on a two-degree-of-freedom planar parallel manipulator provided with kinematic redundancy with the purpose of improving machine accuracy by considering the error inherent to link deformations. Weihmann et al. [11] meticulously investigated the force capabilities of kinematically redundant planar parallel manipulators using an evolutionary algorithm called differential evolution (DE). Ruiz et al. [12] experimentally demonstrated that the energy consumption in the 3-PRRR parallel manipulator is considerably lower than that employed by its non-redundant 3-RRR counterpart using a redundancy resolution scheme based on the Model Predictive Control method. Baron et al. [13] proposed a geometric method capable of avoiding singularities in kinematically redundant planar parallel manipulators based on determining the proximity of the manipulator to a singularity and subsequently optimizing the degrees of freedom according to the final pose of the moving platform. Boudreau [14] introduced a methodology to obtain the wrench capabilities of a kinematically redundant planar parallel manipulator using a wrench polytope approach in which different wrench possibilities like force analysis, the maximum force for a prescribed moment, the maximum reachable force, and the maximum moment with a prescribed force are contemplated, finding explicit solutions to three of these problems. Arsenault et al. [15] developed an algorithm to computing the wrench set of a 3-RPRR planar parallel manipulator including performance indices for diverse applications. It is noteworthy how the kinematic redundancy reaches unlimited levels in the so-called continuum robots [16].

Overall, the development of robotic manipulators with additional degrees of freedom is a research field whose benefits may ameliorate the disadvantages of their non-redundant counterparts. In this work, the concept of similar motions is introduced and applied by handling the kinematic redundancy of planar parallel manipulators. The method is tested on a planar parallel manipulator with five degrees of freedom. To this end, the remaining of the contribution is structured as

follows. In section 2, the topology of the kinematically redundant parallel manipulator and its non-redundant original manipulator is explained. Later on, the displacement analysis is approached in section 3 assuming that the data of the extra degrees of freedom are known a priori. The forward displacement analysis is reduced into three quadratic equations which are solved by resorting to the Sylvester dialytic method of elimination. Meanwhile, the inverse displacement analysis is conducted to obtain individual quadratic equations for two limbs and a direct solution for the third limb. In section 4, the instantaneous kinematics of the robot is addressed by applying the theory of screws. The input-output equation of velocity is systematically obtained without computing the passive joint rates owing to the handling of the properties of reciprocal lines via the Klein form. The concept of similar motions emerges then as an option to avoid the use of the pseudo-inverse Jacobian matrix. Afterwards, the method is proved solving several numerical examples in section 5. Finally, some conclusions are given at the end of the contribution.

2. Description of the robot manipulator

Choosing a non-redundant planar parallel manipulator and adding links as well as actuated kinematic joints to the original mechanism is a natural and effective strategy to generate a kinematically redundant parallel manipulator with capabilities superior to its non-redundant counterpart. The usefulness of kinematic redundancy lies in the fact that it introduces outstanding advantages such as increased workspace, elimination of singularities, improved manipulability and obstacle avoidance, which closes the gap between parallel manipulators and their serial counterparts. Following this fashion, in the paper the chosen non-redundant mechanism to generate a kinematically redundant parallel manipulator is a three-legged parallel robot equipped with two rotational and one translational degree of freedom. The combination of rotary and translational actuators provides interesting advantages in the handling of the Jacobian matrix of manipulators, for example in the reduction of singular configurations [17].

2.1. The non-redundant planar parallel manipulator

Fig. 1 shows a planar parallel manipulator composed of a moving platform m, endowed with an end-effector e, linked to the fixed platform 0 using three limbs numbered 1, 2, and 3. The limbs 1 and 2 are kinematic chains of the $\underline{\text{R}}$RR-type while the central limb 3 is of the R$\underline{\text{P}}$R-type. The actuated joints are underlined.

To explain the notation of the geometry of the manipulator, let us consider that O_XYZ is a reference frame attached to the fixed platform where the origin O is at the nominal position of the lower revolute joint of the central limb. The revolute joints of limbs 1 and 2 are characterized by points A_i, B_i, and C_i for i=1,2. These points are located, respectively, by vectors $\boldsymbol{a}_i$, $\boldsymbol{b}_i$, and $\boldsymbol{c}_i$. Dealing with the

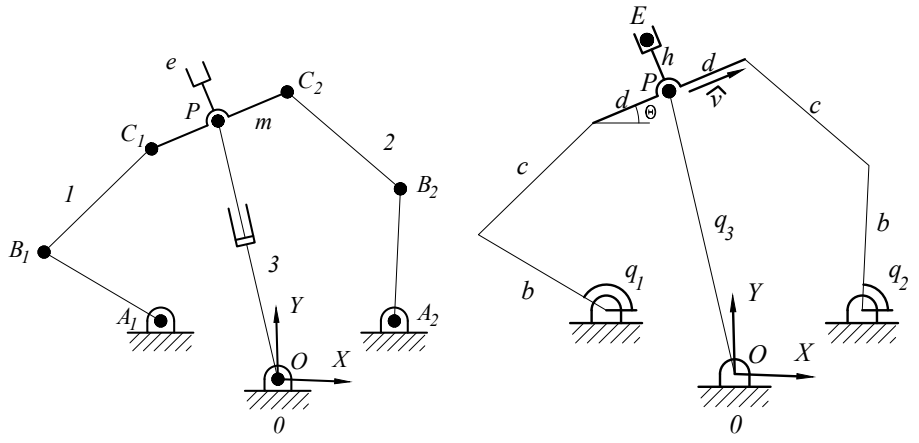

(a) Topology (b) Dimensional parameters and coordinates

Fig. 1. 2RRR+RPR planar parallel manipulator

limb 3, P denotes the point associated to the revolute joint connecting the moving platform to the central limb and located by vector $\boldsymbol{p}$ while E is the point of interest of the gripper or end-effector e that is located by vector $\boldsymbol{e}$. The link lengths are denoted by parameters b, c, and d while h is an offset between points P and E. The unit vector $\hat{\boldsymbol{v}}$ is used to specify the orientation of the moving platform. Hence, the pose of the moving platform m, position and orientation, may be determined by the coordinates of point P and the unit vector $\hat{\boldsymbol{v}}$. That is to say, the position of the moving platform is specified by point P while the orientation is defined by the angle θ which defines the vector $\hat{\boldsymbol{v}}$. The three degrees of freedom of the parallel manipulator, specified by generalized coordinates $q_i (i = 1 \sim 3)$, are established in such a way that the lower revolute joints of limbs 1 and 2 are actuated as well as the prismatic joint. This actuation scheme is governed by one of the basic principles of parallel manipulators: the servomotors are assembled near to the fixed platform. The 2RRR+RPR parallel manipulator shown in Fig. 1 has the virtue that with this topology the moving platform m is able to adopt arbitrary poses as observed from the fixed platform. However, since the number of degrees of freedom of the mechanism is equal to those strictly required to manipulate the moving platform in a three-dimensional task space, then the parallel manipulator is confined to the widely discussed limitations of parallel manipulators. These deficiencies are ameliorated by the introduction of kinematic redundancy to the robot manipulator.

2.2. The kinematically redundant planar parallel manipulator

Although the manipulator of Fig. 1 has the exact number of degrees of freedom required for the moving platform m to adopt arbitrary poses with respect to the fixed platform 0, limited workspace and poor manipulability are marked shortcomings of this type of manipulator. Moreover, as occur for most parallel manipulators, the

threat of singular configurations is usually persistent. To moderate these drawbacks, during the last years a class of robots named kinematically redundant parallel manipulators has been introduced. The kinematic redundancy is achieved through the inclusion of additional kinematic pairs which provides additional degrees of freedom to the existing ones of the complex mechanism.

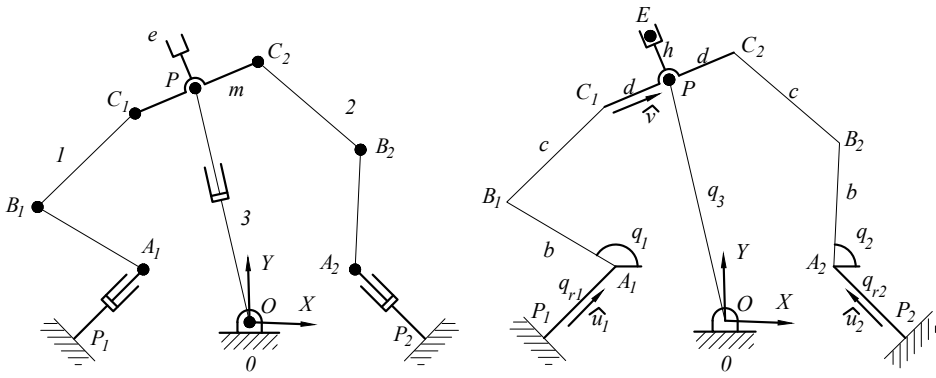

(a) Topology (b) Dimensional parameters and coordinates

Fig. 2. A kinematically redundant planar parallel manipulator

In the contribution, the addition of two actuated prismatic pairs with associated generalized coordinates q_{r1} and q_{r2}, see Fig. 2, with constant orientating unit vectors $\hat{\boldsymbol{u}}_1$ and $\hat{\boldsymbol{u}}_2$ to the 2RRR+RPR parallel manipulator generates a kinematically redundant (3+2) planar parallel manipulator notated as 2PRRR+RPR. The parameters of the mechanism are complemented with points P_1 and P_2 located by vectors $\boldsymbol{p}_1$ and $\boldsymbol{p}_2$, respectively, associated to the extra prismatic joints. With the additional degrees of freedom the mobility of the mechanism is improved and thus we obtain important benefits, for example, an unlimited number of solutions for the inverse kinematics of the manipulator are available. In the paper, the kinematic redundancy is used by assigning motions as close as possible to those assigned to the moving platform.

3. Displacement analysis

The aim of the displacement analysis is to determine analytical expressions to specify the configuration of a manipulator according to the parameters and generalized coordinates that are part of it meeting specific tasks or following given generalized coordinates. In a kinematically redundant parallel manipulator, such as the one studied in the paper, the available degrees of freedom exceed those strictly necessary to control the robot motion, which leads to an obvious benefit in terms of workspace and manipulability, among other topics. In the contribution, it is assumed a priori that the two additional degrees of freedom are known, both for the forward and the inverse position analysis.

3.1. Elementary closure equations

Let us consider that the pose of the moving platform may be expressed using components $w_i (i = 1 \sim 3) \in \mathbb{R}$ as follows [18]

$$\boldsymbol{p} = w_1 \hat{\boldsymbol{i}} + w_2 \hat{\boldsymbol{j}}, \quad \hat{\boldsymbol{v}} = \frac{1 - w_3^2}{1 + w_3^2} \hat{\boldsymbol{i}} + \frac{2w_3}{1 + w_3^2} \hat{\boldsymbol{j}}, \quad \theta = 2 \arctan w_3 \,. \tag{1}$$

The coordinates of points A_1 and A_2 are related to the generalized coordinates q_{ri} and q_{r2} as follows

$$\boldsymbol{a}_i = \boldsymbol{p}_i + q_{ri} \hat{\boldsymbol{u}}_i \quad i = 1, 2 \,. \tag{2}$$

Afterwards, the vectors $\boldsymbol{c}_1$ and $\boldsymbol{c}_2$ may be expressed as

$$\boldsymbol{c}_1 = \boldsymbol{p} - d\hat{\boldsymbol{v}}, \quad \boldsymbol{c}_2 = \boldsymbol{p} + d\hat{\boldsymbol{v}} \,. \tag{3}$$

With this notation, the closure equations of the displacement analysis are formulated using usual vector procedures. Two closure equations can be stated regarding the two links of length c as follows

$$(\boldsymbol{c}_i - \boldsymbol{b}_i) \cdot (\boldsymbol{c}_i - \boldsymbol{b}_i) = c^2 \quad i = 1, 2 \,, \tag{4}$$

where

$$\boldsymbol{b}_i = \boldsymbol{a}_i + b(\cos q_i \hat{\boldsymbol{i}} + \sin q_i \hat{\boldsymbol{j}}) \quad i = 1, 2 \,. \tag{5}$$

Similarly, from the central limb it follows that

$$\boldsymbol{p} \cdot \boldsymbol{p} = q_3^2 \,. \tag{6}$$

Expressions (2)-(6) are simple and yet are valid to solving both, the forward and the inverse position analyses.

3.2. Forward position analysis

The forward position analysis problem of parallel manipulators usually leads to multiple solutions given the nature of the closure equations involved. Thus, a consistent formulation of the direct position analysis problem is crucial to obtain efficient solution methods. For the parallel manipulator at hand, the forward position analysis is formulated as follows. Given a set of generalized coordinates $q_i (i = 1 \sim 5)$ it is required to compute the pose of the moving platform, i.e., it is required to compute the coordinates of point P as well as the orientation of the moving

platform through the compiutation of the unit vector $\hat{\boldsymbol{v}}$ and the angle θ. In that concern, once the pose of the moving platform is computed, the coordinates of any point of the moving platform may be computed, for example the coordinates of point E.

After a few computations, Eqs. (4) and (6) yield three quadratic equations in the unknowns $w_i (i = 1 \sim 3)$. This non-linear system of equations is solved using the Sylvester dialytic method of elimination [19]. The method yields up to eight different poses of the moving platform, real and complex. However, as it is pointed out by one of the reviewers, two of them are spurious solutions and therefore there are at most six solutions for the forward position analysis. Naturally, only the real solutions must be taken into account. Once the unknowns $w_i (i = 1 \sim 3)$ are computed, the pose of the moving platform is obtained by applying Eqs. (2). Furthermore, the coordinates of point E are computed considering that

$$\boldsymbol{e} = \boldsymbol{p} + h\hat{\underline{\boldsymbol{v}}}\,, \tag{7}$$

where $\hat{\underline{\boldsymbol{v}}}$ is a unit vector normal to $\hat{\boldsymbol{v}}$.

3.3. Inverse position analysis

While the forward position analysis is fundamental in the design process of a manipulator, the inverse position analysis is fundamental in the performance of it. On the other hand, to control the performance of the robot, in the forward kinematics the five generalized coordinates must be actuated using specific tasks. The same is not necessarily obligatory for the inverse kinematics.

The inverse position analysis is formulated as follows. Given the coordinates of points P, A_1, and A_2 as well as the unit vector $\hat{\boldsymbol{v}}$ it is required to compute the generalized coordinates $q_i (i = 1 \sim 3)$. In other words, given $w_i (i = 1 \sim 3)$, it is required to compute $q_i (i = 1 \sim 3)$. Firstly, the vectors $\boldsymbol{b}_i$ and $\boldsymbol{c}_i$ are obtained according to Eqs. (5) and (3). Afterwards, by resorting to Eqs. (4) one obtains that

$$k_{i1} \cos q_i + k_{i2} \sin q_i = k_{i3} \quad i = 1, 2\,, \tag{8}$$

where the coefficients $k_{ij} (i = 1, 2; j = 1, 2, 3)$ are computed based on the parameters of the mechanism and the given values $w_i (i = 1 \sim 3)$. After a few computations, from Eqs. (8) we obtain two quadratic equations as follows

$$(k_{i1}^2 + k_{i2}^2) \sin^2 q_i - 2k_{i2}k_{i3} \sin q_i - k_{i1}^2 + k_{i3}^2 = 0\,. \tag{9}$$

Hence, there are two feasible values for each one of the generalized coordinates q_1 and q_2. On the other hand, the generalized coordinate q_3 is computed upon Eq. (6). Of course the argument that the number of solutions of the inverse position analysis is unlimited holds since beyond the translational motion condition of q_{r1} and q_{r2}, there are no limitations on the values assigned to these two generalized coordinates. Thus, the paper introduces the concept of similar motions.

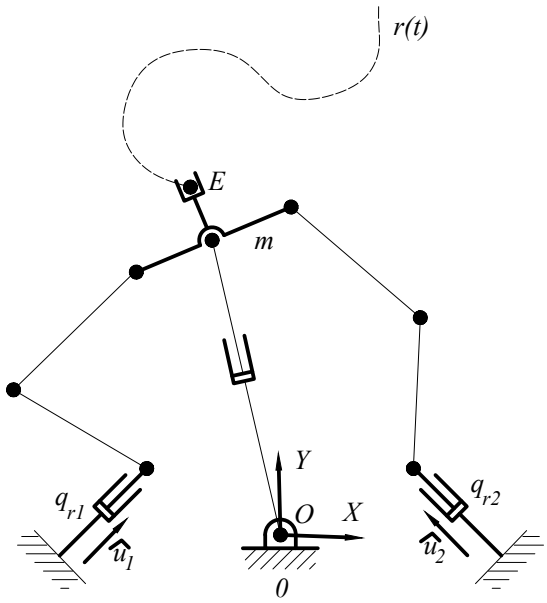

Fig. 3. Path planning trajectory for point E

Let us consider that a specific trajectory $r(t) = x(t)\hat{\boldsymbol{i}} + y(t)\hat{\boldsymbol{j}}$ is assigned to point E of the moving platform as observed from the fixed platform, see Fig. 3. That is to say, the rotation and translation of the moving platform are not arbitrary but must follow a previously defined behaviour. Since there are no specific conditions for the generalized coordinates q_{r1} and q_{r2}, then assuming that the manipulator is in a non-singular posture, trajectories as similar as possible to those assigned to the moving platform can be assigned, thus ensuring to some extent the success of the task assigned to the robot. Naturally, the linear motions of q_{r1} and q_{r2} must be taken into proper account. For example, if the orientation of the moving platform is kept constant and the horizontal motion of q_{r1} and q_{r2} is prioritized, then these generalized coordinates can follow trajectories similar to E given by

$$\boldsymbol{q}_{ri} = \left(\hat{\boldsymbol{i}} + \frac{\hat{\boldsymbol{u}}_i \cdot \hat{\boldsymbol{j}}}{\hat{\boldsymbol{u}}_i \cdot \hat{\boldsymbol{i}}}\hat{\boldsymbol{j}}\right) x(t) \quad i = 1, 2\,. \tag{10}$$

Similarly, if the vertical motion of q_{r1} and q_{r2} is prioritized then it follows that

$$\boldsymbol{q}_{ri} = \left(\frac{\hat{\boldsymbol{u}}_i \cdot \hat{\boldsymbol{i}}}{\hat{\boldsymbol{u}}_i \cdot \hat{\boldsymbol{j}}}\hat{\boldsymbol{i}} + \hat{\boldsymbol{j}}\right) y(t) \quad i = 1, 2\,. \tag{11}$$

Finally, it should be noted that combinations of (10) and (11) are also available.

4. Instantaneous kinematics

The velocity analysis of the parallel manipulator is performed by applying the screw theory [20] which is isomorphic to motor algebra [21] and the Lie algebra $se(3)$ of the Euclidean Group $SE(3)$ [22]. Screw theory is a mathematical tool that focuses on the algebraic calculation of pairs of vectors which are known as dual vectors, classical examples of these inseparable uples are angular velocity with linear velocity and force with momentum. Screw theory is an elegant tool for elucidating problems arising in rigid body kinematics and dynamics. In that concern, the applications of screw theory in the kinematic and dynamic analysis of robotic manipulators is simply outstanding. It should be noted that screw theory bears an extreme relationship to Plücker's line geometry [23] even though a line is a geometrical concept that has no pitch. For example, the pair of vectors that form the Plücker coordinates of a line define a screw whose angular component is a unit vector.

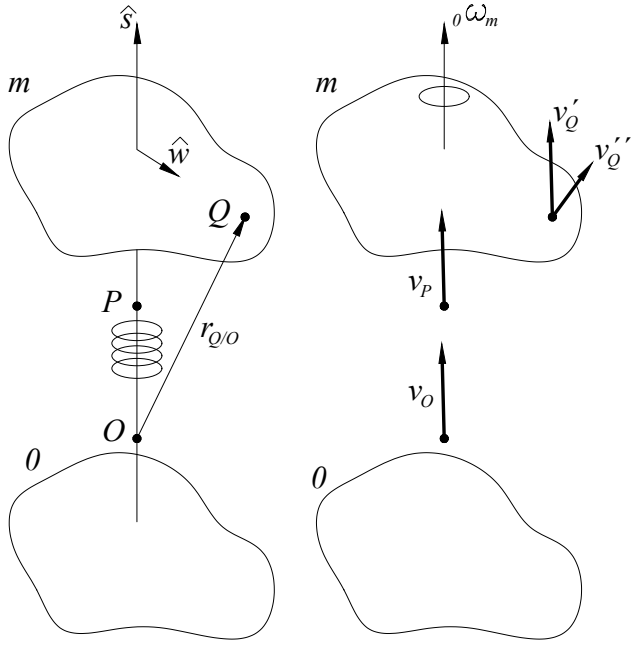

Fig. 4. Rigid body motion and its representation with a helical pair

Let us consider a rigid body m in motion with respect to another body or reference frame 0, see Fig. 4, where ${}_0\omega_m$ denotes the magnitude of the angular velocity vector ${}^0\boldsymbol{\omega}^m$ of body m as measured from body 0. Furthermore, let us consider that bodies m and 0 are connected through a helical pair where the helical pair may be considered as a screw of pitch h. The axis of the screw is along the

unit vector $\hat{\boldsymbol{s}}$ and it is designated as the Instantaneous Screw Axis (ISA). Thus

$$^{0}\boldsymbol{\omega}^{m} = {}_{0}\omega_{m}\,\hat{\boldsymbol{s}}\,. \tag{12}$$

In screw theory, the lead and the pitch are both equal and therefore the angular velocity vector $^{0}\boldsymbol{\omega}^{0}$ and the velocity vector $\boldsymbol{v}_O$ of a point O on the ISA are related by the pitch as follows

$$\boldsymbol{v}_O = h\,{}^{0}\boldsymbol{\omega}^{m}\,. \tag{13}$$

Let us consider that P is another point on the ISA in such a way that $P \neq O$. The velocity of P may be obtained upon the velocity of point O as follows

$$\boldsymbol{v}_P = \boldsymbol{v}_O + {}^{0}\boldsymbol{\omega}^{m} \times \boldsymbol{r}_{P/O}\,, \tag{14}$$

where $\boldsymbol{r}_{P/O}$ is the relative position vector between P and O. However, $\boldsymbol{r}_{P/O} = r_{P/O}\hat{\boldsymbol{s}}$. Hence

$$\boldsymbol{v}_P = \boldsymbol{v}_O + ({}_{0}\omega_{m}\,\hat{\boldsymbol{s}}) \times (r_{P/O}\hat{\boldsymbol{s}}) = \boldsymbol{v}_O = \boldsymbol{v}\,. \tag{15}$$

This result shows that the points on the ISA have the same velocity $\boldsymbol{v}$. On the other hand, let us consider that Q is a point outside of the ISA. Moreover, let us consider that $\hat{\boldsymbol{w}}$ is a unit vector perpendicular to the unit vector $\hat{\boldsymbol{s}}$ and directed to Q. Thus, the position vector $\boldsymbol{r}_{Q/O}$ of point Q with respect to O may be expressed as

$$\boldsymbol{r}_{Q/O} = \lambda_s\hat{\boldsymbol{s}} + \lambda_w\hat{\boldsymbol{w}}\,, \tag{16}$$

where $\lambda_s, \lambda_w \in \mathbb{R}$ are the projections of vector $\boldsymbol{r}_{Q/O}$ in the $\hat{\boldsymbol{s}}\hat{\boldsymbol{w}}$-plane. The velocity vector $\boldsymbol{v}_Q$ of point Q may be obtained considering the conditions of point O as follows

$$\boldsymbol{v}_Q = \boldsymbol{v}_O + {}^{0}\boldsymbol{\omega}^{m} \times \boldsymbol{r}_{Q/O} \tag{17}$$

or

$$\boldsymbol{v}_Q = \boldsymbol{v} + {}_{0}\omega_{m}\hat{\boldsymbol{s}} \times (\lambda_s\hat{\boldsymbol{s}} + \lambda_w\hat{\boldsymbol{w}})\,. \tag{18}$$

Hence

$$\boldsymbol{v}_Q = \boldsymbol{v} + {}_{0}\omega_{m}\lambda_w(\hat{\boldsymbol{s}} \times \hat{\boldsymbol{w}}) \tag{19}$$

and

$$\boldsymbol{v}_Q \cdot \hat{\boldsymbol{w}} = (\boldsymbol{v} + {}_{0}\omega_{m}\lambda_w(\hat{\boldsymbol{s}} \times \hat{\boldsymbol{w}})) \cdot \hat{\boldsymbol{w}} = 0\,. \tag{20}$$

This results show that given an arbitrary point Q of body m, its velocity vector $\boldsymbol{v}_Q$ has two components: i) one component $v'_Q = \boldsymbol{v}$ parallel to the ISA or vector $\hat{\boldsymbol{s}}$, and ii) one component $v''_Q = {}_{0}\omega_{m}\lambda_w$ normal to the $\hat{\boldsymbol{s}}\hat{\boldsymbol{w}}$-plane. Furthermore, the component of velocity of point Q perpendicular to the ISA vanishes.

Theorem 1 *Chasles' Theorem. In kinematics, the Chasles' Theorem (also called the Mozzi-Chasles Theorem) states that the general motion of a rigid body in space can be formally represented by a rotation along a line designated as the Instantaneous Screw Axis (ISA) endowed by a translation along a line parallel to the ISA.*

It is worth mentioning that there is some disagreement about the credits of Chasles' theorem, for details see Ceccarelli [24].

The twist about a screw of rigid body, or velocity state in contemporaneous kinematics, is a six-dimensional vector formed with the linear and angular velocity vectors of the rigid body. The angular velocity is a property of the rigid body and therefore affects any point of the body equally. The linear velocity, on the other hand, depends on the point of the body over which the motion is to be characterized. This point of interest is known as the reference pole. The union of both vectors is indissoluble even though they can be considered as independent concatenated vectors. The representation of the velocity state as the linear combination of screws representing the kinematic pairs connecting the links of kinematic chains is one of the highlights of screw theory whose applications have been of significant relevance in robot kinematics. In a planar parallel manipulator, there are restrictions that limit the mobility of the mechanism and therefore the velocity state of the moving platform is composed of some null elements, in this case two rotations and one translation. Under this scenario, apparently the advantages of the screw theory are diluted and oblige a tedious handling of the Jacobian matrices due to the need to satisfy algebraic requirements associated to the deficient rank of these matrices. This drawback can be ameliorated with the introduction of fictitious kinematic pairs generating square Jacobian matrices. With this in mind, the 2PRRR+RPR is modified as a 2*R*PRR*P*R+RP*S*R parallel manipulator, see Fig. 5a, where *R*, *P*, and *S* are fictitious kinematic pairs. Furthermore, the infinitesimal screws of the robot manipulator are shown in Fig. 5b.

The velocity state of the moving platform m, assuming that the fixed platform 0 is the reference body and O is the reference pole, notated as ${}^{0}\boldsymbol{V}_{O}^{m}$ may be expressed using the infinitesimal screws ${}^{j}\$_{i}^{j+1}(i = 1, 2, 3; j = 0 \sim 5)$ as linear superposition combinations according to the joint rates ${}_{j}\omega_{j+1}^{i}(i = 1, 2, 3; j = 0 \sim 5)$ of the planar parallel manipulator as follows

$$\sum_{j=0}^{j=5} {}_{j}\omega_{j+1}^{i}\, {}^{j}\$_{i}^{j+1} = {}^{0}\boldsymbol{V}_{O}^{m} \quad i = 1, 2, 3\,, \tag{21}$$

where ${}_{1}\omega_{2}^{1} = \dot{q}_{r1}$, ${}_{2}\omega_{3}^{1} = \dot{q}_{1}$, ${}_{1}\omega_{2}^{2} = \dot{q}_{r2}$, ${}_{2}\omega_{3}^{2} = \dot{q}_{2}$, and ${}_{1}\omega_{2}^{3} = \dot{q}_{3}$ are the generalized speeds. Meanwhile, owing to the condition of fictitious kinematic pair it follows that the joint rates ${}_{0}\omega_{1}^{1}$, ${}_{4}\omega_{5}^{1}$, ${}_{0}\omega_{1}^{2}$, ${}_{4}\omega_{5}^{2}$, ${}_{2}\omega_{3}^{3}$, ${}_{3}\omega_{4}^{3}$, and ${}_{4}\omega_{5}^{3}$ vanish.

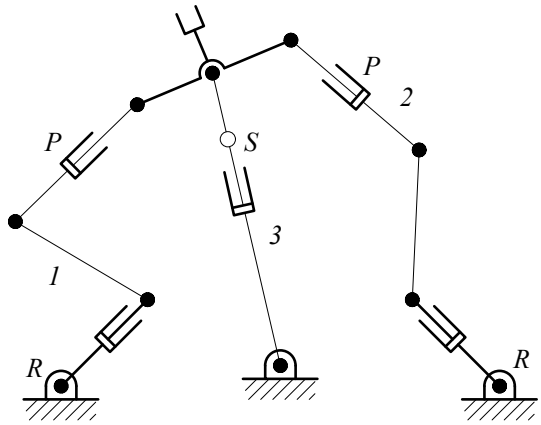

(a) Fictitious kinematic pairs

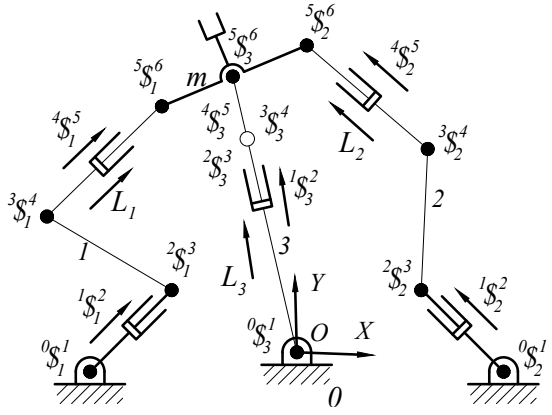

(b) Infinitesimal screws and reciprocal lines

Fig. 5. Modified parallel manipulator

Equation (21) can be concisely written in matrix form as follows

$$\bar{\mathbf{J}}_i \, \Omega_i = {}^0\boldsymbol{V}_O^m \quad i = 1, 2, 3\,, \tag{22}$$

where

$\bar{\mathbf{J}}_i = \left[{}^0\$_i^1 \quad {}^1\$_i^2 \quad {}^2\$_i^3 \quad {}^3\$_i^4 \quad {}^4\$_i^5 \quad {}^5\$_i^6 \right]$ is the local Jacobian matrix of the $i-$th limb,

$\Omega_i = \left[{}_0\omega_1^i \quad {}_1\omega_2^i \quad {}_2\omega_3^i \quad {}_3\omega_4^i \quad {}_4\omega_5^i \quad {}_5\omega_6^i \right]^T$ is the joint rates matrix of the $i-$th limb,

${}^0\boldsymbol{V}_O^m = \left[0 \quad 0 \quad \omega_Z \quad v_X \quad v_Y \quad 0 \right]^T$.

The insertion of passive joint rates in the Eq. (22) implies an inefficient use of it in the velocity analysis of the parallel manipulator. Furthermore, the forward

velocity analysis cannot be performed since, in that formula, all the joint rates of the manipulator are required, while in the inverse analysis there are self motions in the limbs due to kinematic redundancy. The elimination of passive joint rates is a key task in obtaining an efficient input-output equation of velocity of the robot. In that concern, the Klein form of the Lie algebra $se(3)$ of the Euclidean group $SE(3)$, notated as $\{*;*\}$, is a mathematical operation recurrently employed in parallel manipulators.

Let us consider three lines L_1, L_2, and L_3 in Plücker coordinates as shown in Fig. 5b. Applying the Klein form of the line L_1 to the velocity state in screw form of limb 1, with term reduction, leads to

$$\{L_1; {}^0\boldsymbol{V}_O^m\} = \dot{q}_{r1}\{L_1; {}^1\$_1^2\} + \dot{q}_1\{L_1; {}^2\$_1^3\}\,. \tag{23}$$

Analogously, from limbs 2 and 3 we generate expressions given by

$$\{L_2; {}^0\boldsymbol{V}_O^m\} = \dot{q}_{r2}\{L_2; {}^1\$_2^2\} + \dot{q}_2\{L_2; {}^2\$_2^3\} \tag{24}$$

and

$$\{L_3; {}^0\boldsymbol{V}_O^m\} = \dot{q}_3\,. \tag{25}$$

On the other hand, owing to the constrained rotations of the moving platform there are two reciprocal system L_4 and L_5 to the velocity state ${}^0\boldsymbol{V}_O^m$ given by

$$L_4 = \begin{bmatrix} \boldsymbol{0} \\ \hat{\boldsymbol{i}} \end{bmatrix}, \quad L_5 = \begin{bmatrix} \boldsymbol{0} \\ \hat{\boldsymbol{j}} \end{bmatrix}\,. \tag{26}$$

The reciprocal systems L_4 and L_5 refer that the moving platform cannot rotate, respectively, about the X and Y axes. Furthermore, a third reciprocal system L_6 associated to the constrained displacement of the moving platform may be considered as follows

$$L_6 = \begin{bmatrix} \hat{\boldsymbol{k}} \\ \boldsymbol{0} \end{bmatrix}\,. \tag{27}$$

Thus, based on the Klein form it follows that

$$\{L_i; {}^0\boldsymbol{V}_O^m\} = 0 \quad i = 4, 5, 6\,. \tag{28}$$

The cancellation of passive joint rates allows us to sort in a matrix-vector form Eqs. (23), (24), (25), and (28), as follows

$$\mathrm{Jv}^T \,\Delta\, {}^0\boldsymbol{V}_O^m = \mathrm{Jq}\,\boldsymbol{\dot{Q}}\,, \tag{29}$$

where

$\mathrm{Jv} = \begin{bmatrix} L_1 & L_2 & L_3 & L_4 & L_5 & L_6 \end{bmatrix}$ is the Jacobian matrix of the moving platform,

$$\mathrm{Jq} = \begin{bmatrix} \{L_1; {}^1\$_1^2\} & 0 & \{L_1; {}^2\$_1^3\} & 0 & 0 \\ 0 & \{L_2; {}^1\$_2^2\} & 0 & \{L_2; {}^2\$_2^3\} & 0 \\ 0 & 0 & 0 & 0 & 1 \\ 0 & 0 & 0 & 0 & 0 \\ 0 & 0 & 0 & 0 & 0 \\ 0 & 0 & 0 & 0 & 0 \end{bmatrix}$$ is the Jacobian matrix of generalized speeds,

$\boldsymbol{Q} = \begin{bmatrix} \dot{q}_{r1} & \dot{q}_{r2} & \dot{q}_1 & \dot{q}_2 & \dot{q}_3 \end{bmatrix}^T$ is the vector of generalized speeds,

$\Delta = \begin{bmatrix} 0 & \mathrm{I} \\ \mathrm{I} & 0 \end{bmatrix}$ is a six-dimensional polarity operator.

It is noteworthy how the strong geometrical meaning of the screw theory allows one to obtain the Jacobian matrices of the manipulator in a systematic way, and free of passive joint rates.

To solve the forward velocity analysis, Eq. (29) is re-written as follows

$$ {}^0\boldsymbol{V}_O^m = \mathrm{J}\,\boldsymbol{Q}\,. \tag{30}$$

where

$$\mathrm{J} = (\mathrm{Jv}^T\,\Delta)^{-1}\,\mathrm{Jq}\,. \tag{31}$$

Thus, the computation of the matrix J requires that the matrix Jv must be invertible, otherwise the manipulator is in a forward singular configuration. This situation is undesirable and should be properly considered in the design process of the manipulator. For example, in a forward singular configuration the robot gains unforeseen degrees of freedom which makes it uncontrollable. This kind of singularity emerges when $\det \mathrm{Jv} = 0$. Indeed, when the lines L_1, L_2, and L_3, see Fig. 5b, are concurrent or parallel.

On the other hand, to solve the inverse velocity analysis, a typical method is based on the so-called pseudo-inverse Jacobian matrix. To this end, from Eq. (30) one obtains that the vector $\boldsymbol{Q}$ is given by

$$\boldsymbol{Q} = \mathrm{J}^+\,{}^0\boldsymbol{V}_O^m\,, \tag{32}$$

where

$$\mathrm{J}^+ = \mathrm{J}^{\mathrm{T}}(\mathrm{J}\mathrm{J}^{\mathrm{T}})^{-1} \tag{33}$$

is the pseudo-inverse of matrix J [25]. As noted by Faroni et al. [26], the methods of inverse infinitesimal kinematics based on the pseudo-inverse do not provide a

reliable strategy when the manipulator's own limits and constraints are involved. In that sense, their a priori application may result in position, velocity and acceleration limits not being respected. In such a scenario, actuator saturation usually occurs and the consequences are obvious. In addition to such problems, in the manipulator under study it occurs that the J^{+} matrix is singular, which excludes it from its possible use, obviously. There are several methods classified mainly in local and global strategies [27] to circumvent these drawbacks, and several more, without wasting the potential of kinematic redundancy, enhancing the capability of robotic manipulators with such attributes. Faroni et al. [26] implemented a predictive strategy devoted to optimal control of redundant robotic manipulators, resulting in efficient handling of the constraints of the manipulators. Santos and da Silva [28] solved the kinematic redundancy by means of a global optimization based on the gradient projection concept with the objective of applying differential dynamic programming (DDP). Vieira et al. [29] solved the kinematic redundancy by evaluating the probability of falling into singular configurations based on the Monte Carlo method. Wu et al. [30] solved the inverse kinematics of dual robots by addressing redundancy by formulating unified quadratic programming problems combining different optimization criteria, see Kwon et al. [31], with the objective of guaranteeing smooth velocity and acceleration profiles, including the cancellation of the velocity at the end of the motion. Hess-Coelho et al. [32] applied Modular Modeling Methodology to kinematically redundant parallel mechanisms focusing on the derivation of inverse dynamics models in order to test trajectory planning by proposing metrics to evaluate the proximity to singularities and reduce energy consumption.

In this paper, the kinematic redundancy is solved by introducing the concept of *similar motions*. The concept is simple, natural and therefore easy to follow. Once a specific velocity state has been assigned to the moving platform, of course considering point E as the reference pole, the generalized velocities $\dot{q}_{r1}$ and $\dot{q}_{r2}$ follow velocities as close as possible to those imposed on the moving platform. Afterwards, the generalized velocities $\dot{q}_1$, $\dot{q}_2$ and $\dot{q}_3$ are computed using the following expression

$$\boldsymbol{Q}_{123} = \mathrm{M}\, {}^{0}\boldsymbol{V}_{O}^{m} - \mathrm{D}\, \boldsymbol{Q}_{r}\,, \tag{34}$$

where

$$\boldsymbol{Q}_{123} = \begin{bmatrix} \dot{q}_1 & \dot{q}_2 & \dot{q}_3 & 0 & 0 & 0 \end{bmatrix}^{T},$$

$$\boldsymbol{Q}_{r} = \begin{bmatrix} \dot{q}_{r1}\{L_1; {}^{1}\$_1^2\} & \dot{q}_{r2}\{L_2; {}^{1}\$_2^2\} & 0 & 0 & 0 & 0 \end{bmatrix}^{T},$$

$$\mathrm{D} = \mathrm{diag}\begin{bmatrix} 1/\{L_1; {}^{2}\$_1^3\} & 1/\{L_2; {}^{2}\$_2^3\} & 1 & 1 & 1 & 1 \end{bmatrix},$$

$$\mathrm{M} = \mathrm{D}\, \mathrm{Jv}^{T}\, \Delta\,.$$

Hence, we have only one solution for the inverse velocity analysis. Furthermore, the inverse velocity analysis is feasible as long as $\{L_1; {}^2\$_1^3\}, \{L_2; {}^2\$_2^3\} \neq 0$. Otherwise, the parallel manipulator is at an inverse singularity. For example, the inverse velocity analysis is not possible when any of the links of lengths a and b are aligned, of course in the same limb. On the other hand, a combined singularity emerges when we have simultaneously forward and inverse singularities. Examples of singular postures of the manipulator are shown in Fig. 6.

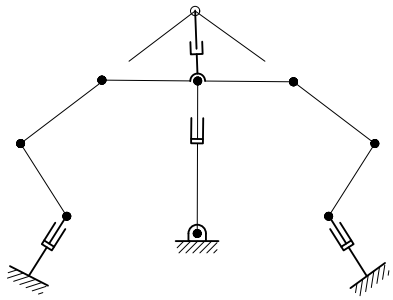

(a) Forward. Concurrent lines

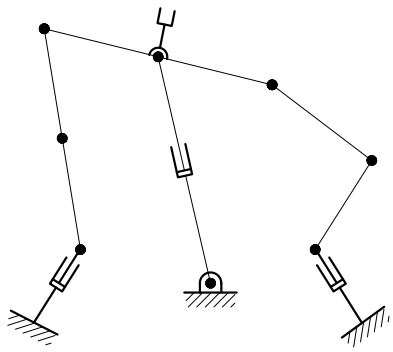

(b) Inverse. Unfolded limb

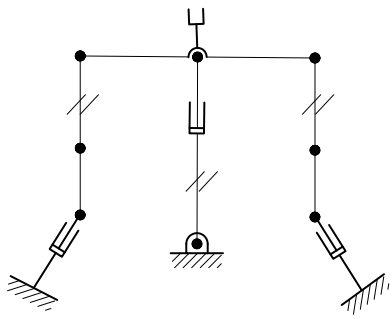

(c) Combined. Parallel lines

Fig. 6. Three singular configurations of the parallel manipulator

It is important to note that even when the manipulator has two additional degrees of freedom, it is not free of singularities.

5. Simulation results

In this section, the performance of the parallel manipulator under study is proved by numerical examples. Owing to the nature of the robotic manipulator, the inverse velocity analysis is discussed in more detail. According to the singularity analysis, a suitable reference configuration free of singularities for the parallel manipulator is shown in Fig. 7. To numerically perform the computation of the kinematic analysis, Maple sheets were elaborated for the required algorithms.

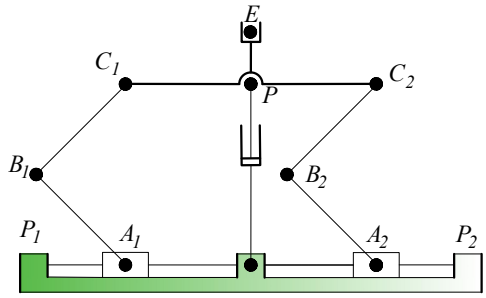

Fig. 7. Reference configuration of the parallel manipulator

The chosen values for the parameters and generalized coordinates of the robot in its reference configuration are listed in Table 1. To complete the information, the nominal coordinates of the limbs are given in Table 2.

Table 1. Parameters and reference configuration of the parallel manipulator

$b = c = d = 100$ [mm], $h = 50$ [mm]
$q_{r1} = q_{r2} = 100$ [mm], $q_1 = q_2 = 3\pi/8$ [rad], $q_3 = 141.421$ [mm]
$\hat{\boldsymbol{u}}_1 = \hat{\boldsymbol{i}}, \hat{\boldsymbol{u}}_1 = -\hat{\boldsymbol{i}}$

Table 2. Coordinates of the limbs in the reference configuration

i	P_i [mm]	A_i [mm]	B_i [mm]	C_i [mm]
1	(−200,0,0)	(−100,0,0)	(−170.710,70.71,0)	(−100,141.421,0)
2	(200,0,0)	(100,0,0)	(29.289,70.71,0)	(100,141.421,0)

Three outstanding features of this configuration are as follows:

1. There are two identical extremities ABC.
2. The vectors $\hat{\boldsymbol{u}}$ are collinear so that the inertias in motion are minimized.
3. The lines L_1, L_2 and L_3 are neither parallel nor concurrent and thus the manipulator is free of singularities.

Example 1. Forward-inverse displacement

To exemplify the forward position analysis, let us consider the data of Table 1. The application of the method yields four real solutions which are listed in Table 3.

Table 3. Solutions of the forward position analysis

sol	w_1	w_2	w_3
1	0	141.421	0
2	−109.008	90.095	−0.506
3	−133.803	45.790	0.394
4	−141.421	0	0

Solution 1 of Table 3 corresponds to the configuration of the robot provided in Fig. 7. To exemplify the inverse position analysis, let us consider that the pose of the moving platform corresponds to solution 3 of Table 3. In this configuration we have that

$$P = (-133.803, 45.790, 0), \quad \hat{\boldsymbol{v}} = 0.73\hat{\boldsymbol{i}} + 0.683\hat{\boldsymbol{j}}\,. \tag{35}$$

The four solutions of the inverse position analysis, provided that $q_{r1} = q_{r2} = 100$ [mm], are listed in Table 4.

Table 4. Solutions of the inverse position analysis

sol.	q_1 [rad]	q_2 [rad]	q_3 [mm]
1	−1.940	2.356	141.421
2	−1.940	2.692	141.421
3	2.356	2.356	141.421
4	2.356	2.692	141.421

Example 2. Forward velocity

To exemplify numerically the forward velocity analysis, let us consider the reference configuration of the robot provided in Fig. 7. Assume that from the reference configuration of the robot, the generalized coordinates are regulated by periodic functions given by

$$\begin{cases} q_{r1} = 100 \sin t \cos t \ \text{[mm]}, \quad q_{r2} = -160 \sin t \cos t \ \text{[mm]} \\ q_1 = -1.25 \sin t \cos t \ \text{[rad]}, \quad q_2 = -1.5 \sin t \cos t \ \text{[rad]}, \quad q_3 = 100 \sin t \cos t \ \text{[mm]} \end{cases}$$

where the time t is given in the interval $0 \leqslant t \leqslant 2\pi$ [s]. With these data, the resulting temporal behaviour of the instantaneous kinematics of the moving platform is provided in Fig. 8. Furthermore, the plots obtained by applying the theory of screws were verified with the aid of special simulation software like ADAMS™.

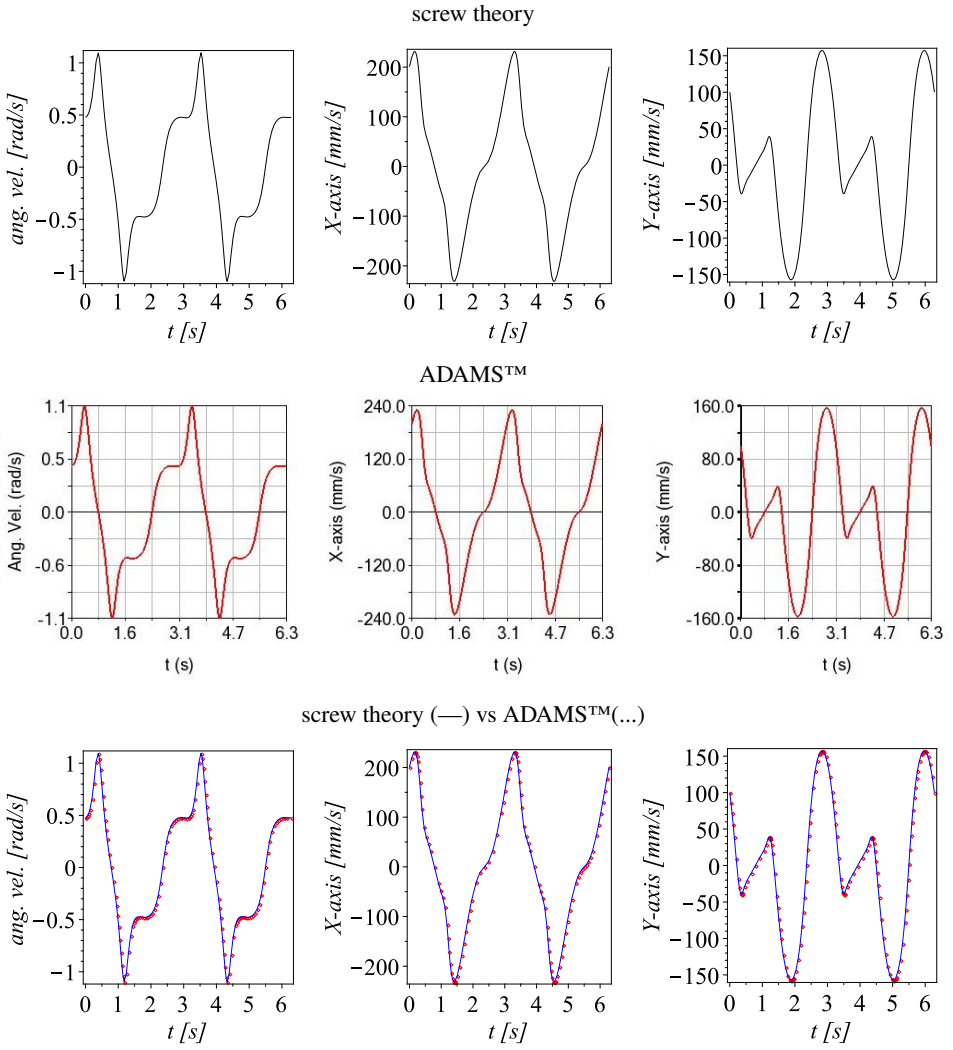

Fig. 8. Example 2. Temporal behaviour of the angular velocity of the moving platform and the velocity of point E

These plots were added in Fig. 8 with the purpose to make a quick comparison of the results obtained using both and quite different methods.

Dealing with example 2, it is worth concluding that according to Fig. 8, the plots obtained with the screw theory are in excellent agreement with the plots generated with ADAMS™.

Example 3. Generation of a straight line

Assume that the manipulator is at its reference configuration. Moreover, suppose that point E of the moving platform must perform a translation given by

$\boldsymbol{e} = 10t\hat{\boldsymbol{i}} - 5t\hat{\boldsymbol{j}}$ [mm] endowed by a rotation specified by the orientating angle $\theta = 0.075t$ [rad] where the time t is restricted to the interval $0 \leqslant t \leqslant 10$ [s]. According to the similar motions method, the generalized speeds of the additional kinematic pairs are chosen as $\dot{q}_{r1} = \dot{q}_{r2} = 10$ [mm/s] in order to replicate the horizontal motion of point E. Thereafter, the time history of the inverse kinematics of the manipulator using the method of the paper is summarized in the plots of Figs. 9 and 10. Furthermore, the plots of the instantaneous kinematics are compared with plots generated with the special software ADAMS™.

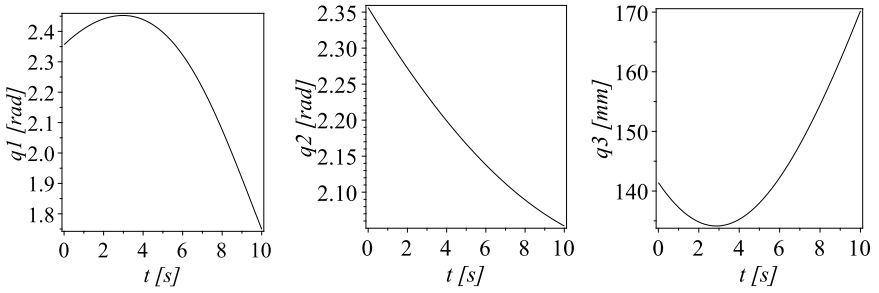

Fig. 9. Example 3. Temporal behaviour of the generalized coordinates q_1, q_2 and q_3

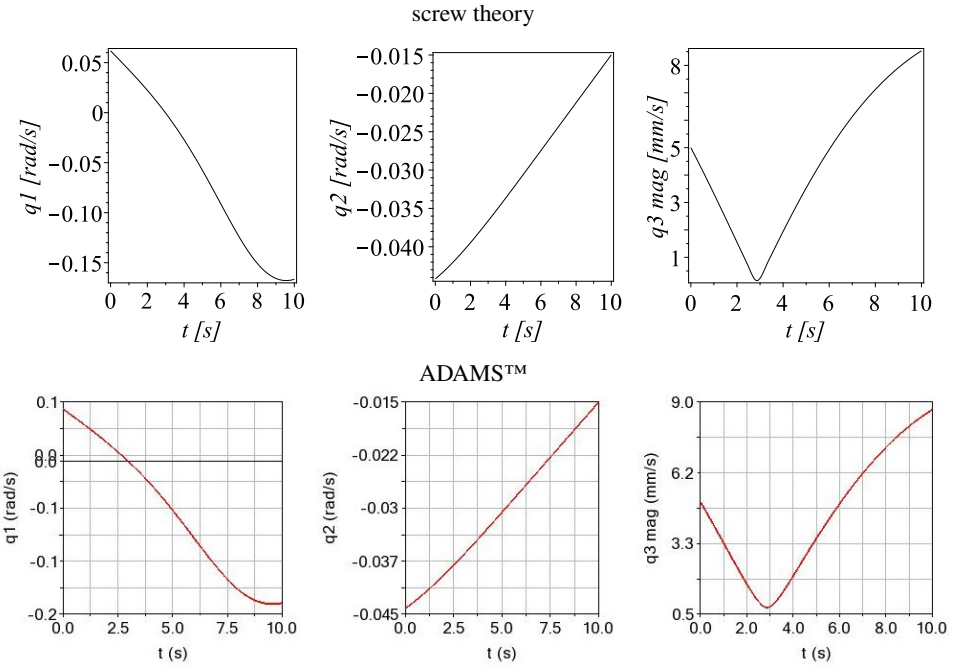

Fig. 10. Example 3. Temporal behaviour of the generalized speeds $\dot{q}_1$, $\dot{q}_2$ and $\dot{q}_3$

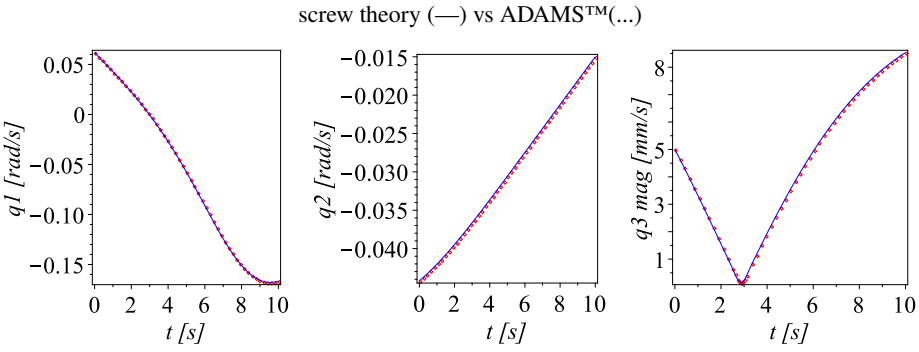

Fig. 10. cont. Example 3. Temporal behaviour of the generalized speeds $\dot{q}_1$, $\dot{q}_2$ and $\dot{q}_3$

Dealing with the generalized speed $\dot{q}_3$, the plot reports the magnitude of the joint rate since ADAMS™ does not accept negative values for the relative velocity of prismatic joints. On the other hand, note how the results of the velocity analysis of example 3 applying the screw theory agree excellently with the plots generated with ADAMS™.

Example 4. Generation of a circle

Consider that from the reference configuration of the robot, see Fig. 7, point E generates a circle of radius 50 [mm] and center with coordinates $(0, 141.421, 0)$ [mm]. The motion of point E is counterclockwise and the moving platform keeps a constant orientation, i.e., $\theta = 0$ [rad]. Moreover, consider that point E starts its motion from rest, both in velocity and acceleration, and after 5 seconds returns to its original position. With these data, it is required to compute the time history of the generalized coordinates meeting the motion conditions imposed to the moving platform. Applying Craig's method [33], it is found that fifth order polynomials are appropriate functions to satisfy the motion conditions imposed to the moving platform. Assuming that $E(t) = (Ex(t), Ey(t), 0)$ [mm], the instantaneous coordinates of point E are obtained as

$$Ex(t) = 50.0\cos(1.570 + .502t^3 - .150t^4 + 0.120e - 1t^5) \tag{36a}$$

$$Ey(t) = 141.421 + 50.0\sin(1.570 + .502t^3 - .150t^4 + 0.120e - 1t^5) \tag{36b}$$

Meanwhile, the velocity vector of point E results to be

$$\boldsymbol{v}_E = -3.015t^2(25-10t+t^2)\sin(1.570+.502t^3-.150t^4+0.120e-1t^5)\hat{\boldsymbol{i}}+ 3.015t^2(25-10t+t^2)\cos(1.570+.502t^3-.150t^4+0.120e-1t^5)\hat{\boldsymbol{j}}\,. \tag{37}$$

For clarity, the time history of point E is provided in Fig. 11.

Therefore, using the criterion of similar motions, the generalized speeds $\dot{q}_{r1}$ and $\dot{q}_{r2}$ are chosen as

$$\dot{q}_{r1} = \dot{q}_{r2} = -3.015t^2(25-10t+t^2)\sin(1.570+.502t^3-.150t^4+0.120e-1t^5)\,. \tag{38}$$

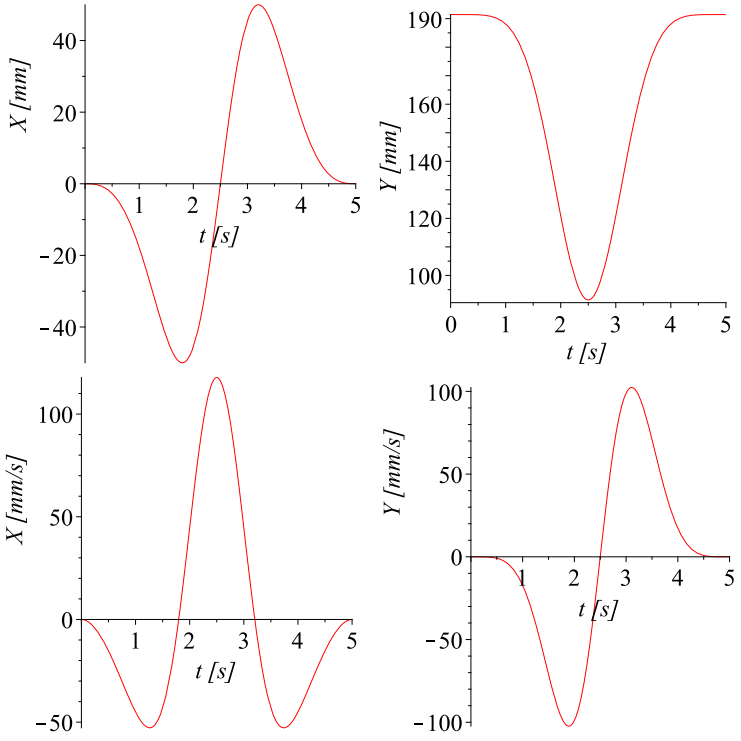

Fig. 11. Example 4. Temporal behaviour of point E

The resulting time history of the generalized coordinates q_1, q_2 and q_3 is depicted in Fig. 12.

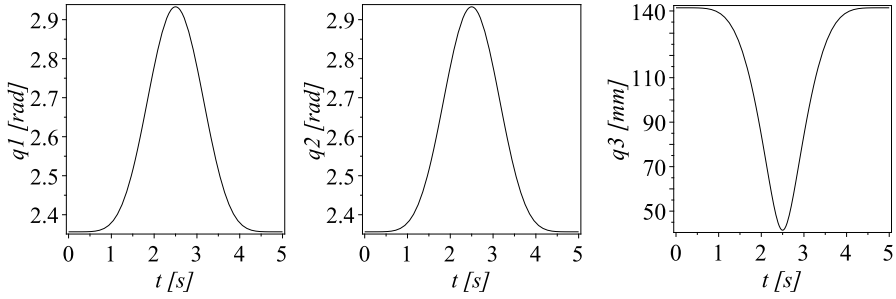

Fig. 12. Example 4. Temporal behaviour of the generalized coordinates q_1, q_2 and q_3

Meanwhile, the resulting time history by applying the theory of screws of the generalized speeds $\dot{q}_1$, $\dot{q}_2$ and $\dot{q}_3$ is provided in Fig. 13.

To verify the results of the velocity analysis, instead of resorting again to the ADAMS™ software, the results of the position analysis are fitted to spline curves by applying the *with(CurveFitting)* library of the Maple software. Thereafter, the

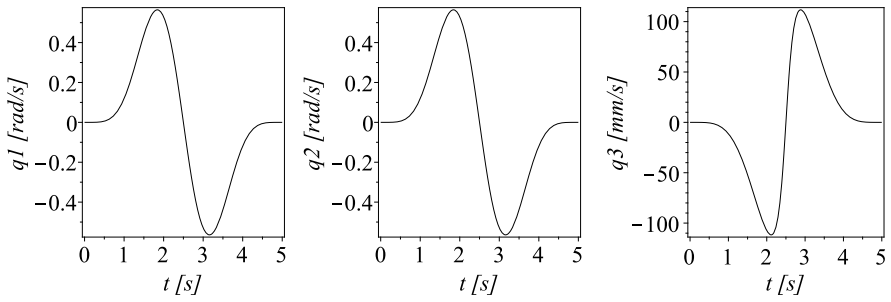

Fig. 13. Example 4. Time history of the generalized speeds $\dot{q}_1$, $\dot{q}_2$ and $\dot{q}_3$ using the theory of screws

time-dependent functions associated with the generalized coordinates q_1, q_2 and q_3 are obtained as

$$q_1 = \begin{cases} 2.356197010+1.572888309e-7t+0.2527111691e-4t^3 & t < 0.1 \\ 2.356+9.154e-7t+0.758e-5(t-.1)^2+0.232e-2(t-.1)^3 & t < 0.2 \\ \vdots & \\ 2.356-0.720e-4t+0.704e-3(t-4.8)^2-0.232e-2(t-4.8)^3 & t < 4.9 \\ 2.356-9.154e-7t+0.758e-5(t-4.9)^2-0.252e-4(t-4.9)^3 & \text{otherwise} \end{cases} \tag{39}$$

$$q_2 = \begin{cases} 2.356197010+1.572888309e-7t+0.2527111691e-4t^3 & t < 0.1 \\ 2.356+9.154e-7t+0.758e-5(t-.1)^2+0.232e-2(t-.1)^3 & t < 0.2 \\ \vdots & \\ 2.356-0.720e-4t+0.704e-3(t-4.8)^2-0.232e-2(t-4.8)^3 & t < 4.9 \\ 2.356-9.154e-7t+0.758e-5(t-4.9)^2-0.252e-4(t-4.9)^3 & \text{otherwise} \end{cases} \tag{40}$$

$$q_3 = \begin{cases} 141.4210000-0.1490542687e-4t-0.2309457313e-2t^3 & t < 0.1 \\ 141.421-0.841e-4t-0.692e-3(t-.1)^2-.212(t-.1)^3 & t < 0.2 \\ \vdots & \\ 141.389+0.659e-2t-0.643e-1(t-4.8)^2+.212(t-4.8)^3 & t < 4.9 \\ 141.420+0.841e-4t-0.692e-3(t-4.9)^2+0.230e-2(t-4.9)^3 & \text{otherwise} \end{cases} \tag{41}$$

Afterwards, the generalized speeds $\dot{q}_1$, $\dot{q}_2$, and $\dot{q}_3$ are determined as the time derivatives of Eqs. (39)-(41). The corresponding plots, and their comparison with

the plots of the velocity analysis applying the screw theory, are provided in Fig. 14. Please note that the outcomes produced by the two methods differ by a margin that is practically negligible.

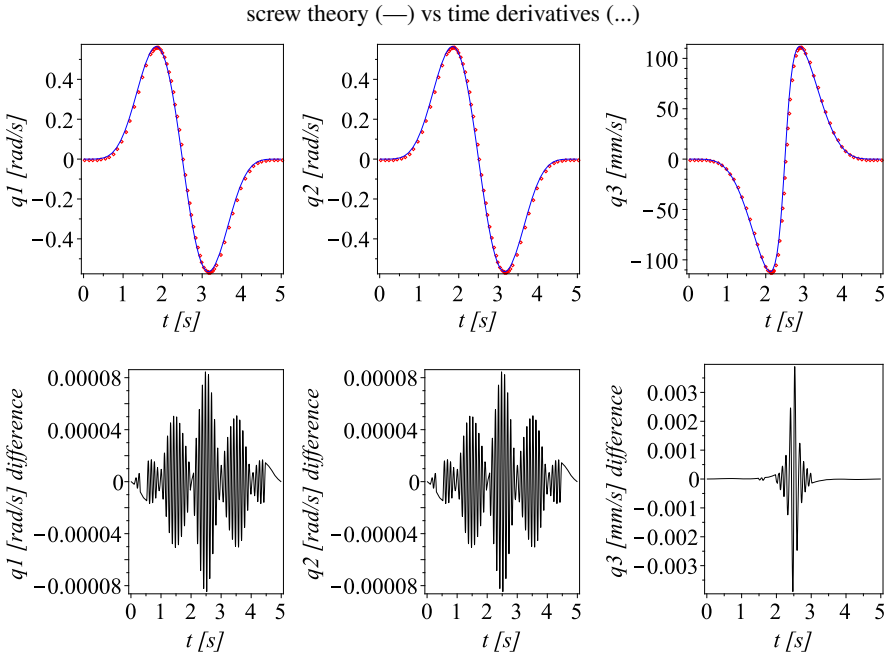

Fig. 14. Example 4. Time history of the generalized speeds $\dot{q}_1$, $\dot{q}_2$ and $\dot{q}_3$

6. Conclusions

It is widely proven and well documented that kinematic redundancy significantly improves the performance of robot manipulators. One of the most interesting points of kinematic redundancy is undoubtedly concentrated in the inverse kinematic analysis since in this case an infinite number of solutions are available and the selection of the best option can be an arduous and complicated task. Vieira et al. [29] approached the kinematic redundancy with the purpose to avoid singularities using the Monte Carlo Simulation and surrogate models. The problem of singularities and their solution using kinematic redundancy is a topic that has been growing in recent years owing to the possibility to increase the workspace [34]. Ginnante et al. [35] introduced a control algorithm in which tasks are prioritized in such a way that an optimization of the robot design is achieved due to the substitution of design parameters by virtual kinematic pairs. In summary, kinematic redundancy has been efficiently resolved by employing, among other strategies, the optimization of suitable performance criteria, the augmentation of the task space, torque minimization, type-synthesis design for decoupling the workspace,

pseudo-inverse Jacobian matrix formulation, optimal force transmission, and so on. However, these methods are often computationally demanding and mathematically complex [28]. In that concern, as noted by Chiaverini et al. [36] there are industrial applications yielding cyclic or repetitive task motion and therefore simpler methods of kinematic redundancy resolution may be employed. Following this option, in this work the kinematic redundancy is approached by considering the topology of a non-redundant planar parallel manipulator and then adding extra kinematic pairs performing similar motions to the desired to the moving platform. The method comprises the following steps:

1. Choose the kinematically redundant joints of the parallel manipulator. Since the manipulator must operate in unexpected scenarios or perform tasks that are not necessarily repetitive but complex, an appropriate choice is to select kinematic pairs that are near to the fixed platform, i.e., kinematic pairs that link the limbs to the fixed platform. This action reduces the inertia in motion and simplifies the kinematic analysis.
2. Assign particular trajectories to the redundant kinematic pairs. With this action, the use of the pseudo-inverse Jacobian matrix is avoided and the inverse kinematic analysis is solved as if one had a non-redundant planar parallel manipulator.
3. The assignment of trajectories is not governed by a particular criterion, which is one of the most representative advantages of the method. One option is to replicate in the redundant kinematic pairs, as far as possible, the trajectories assigned to the moving platform. In a glance, it seems that with this procedure the advantage of having a kinematically redundant manipulator is missed. The doubt is dispelled if one considers that in reality the kinematic pairs are used to move a non-redundant manipulator as a whole to configurations that would be prohibitive without the additional kinematic pairs, thereby increasing the workspace.

The method is applied in a five degrees of freedom planar parallel manipulator free of passive limbs. The kinematic redundancy is concentrated on two prismatic pairs which are added to a non-redundant planar parallel manipulator composed of a moving platform linked to a fixed platform by means of three limbs. The robot topology is designated as 2PRRR+RPR where the active kinematic pairs are underlined. The method of kinematic analysis developed is tested with some numerical examples, with special emphasis on the inverse kinematic analysis of the manipulator owing to the nature of the mechanism under study. Moreover, the most relevant numerical results of the examples are successfully compared with plots generated with the ADAMS™ software.

Finally, as far as the author assumes, the strategy proposed in the paper to solve the kinematic redundancy of planar parallel manipulators has not been considered in previous works. On the other hand, the validation of the numerical results using alternative strategies is a proof of the reliability of the kinematic analysis method presented in the paper, especially the use of the screw theory.

References

[1] J. Baillieul, J. Hollerbach, and R. Brockett. Programming and control of kinematically redundant manipulators. In *The 23rd IEEE Conference on Decision and Control*, pages 768–774, 1984. doi: 10.1109/CDC.1984.272110.

[2] P. Chang. A closed-form solution for inverse kinematics of robot manipulators with redundancy. *IEEE Journal on Robotics and Automation*, 3(5):393–403, 1987. doi: 10.1109/JRA.1987.1087114.

[3] C.A. Klein and B.E. Blaho. Dexterity measures for the design and control of kinematically redundant manipulators. *The International Journal of Robotics Research*, 6(2):72–83, 1987. doi: 10.1177/027836498700600206.

[4] A.A. Maciejewski and C.A. Klein. Numerical filtering for the operation of robotic manipulators through kinematically singular configurations. *Journal of Robotic Systems*, 5(6):527–552, 1988. doi: 10.1002/rob.4620050603.

[5] B. Siciliano and J.-J.E. Slotine. A general framework for managing multiple tasks in highly redundant robotic systems. In *Fifth International Conference on Advanced Robotics 'Robots in Unstructured Environments*, volume 2, pages 1211–1216, 1991. doi: 10.1109/ICAR.1991.240390.

[6] J.A. Kuo and D.J. Sanger. Task planning for serial redundant manipulators:. *Robotica*, 15(1):75–83, 1997. doi: 10.1017/S026357479700009X.

[7] J.P. Karlen and M. Jack. Reflexive obstacle avoidance for kinematically-redundant manipulators, 1989. NASA, report N90-29047.

[8] J. Wang and C.M. Gosselin. Kinematic analysis and design of kinematically redundant parallel mechanisms. *Journal of Mechanical Design*, 126(1):109–118, 2004. doi: 10.1115/1.1641189.

[9] I. Ebrahimi, J.A. Carretero, and R. Boudreau. Kinematic analysis and path planning of a new kinematically redundant planar parallel manipulator. *Robotica*, 26(3):405–413, 2008. doi: 10.1017/S0263574708004256.

[10] Y. Jiang and T.-M. Li and L.-P. Wang. Dynamic modeling and redundant force optimization of a 2-DOF parallel kinematic machine with kinematic redundancy. *Robotics and Computer-Integrated Manufacturing*, 32:1–10, 2015. doi: 10.1016/j.rcim.2014.08.001.

[11] L. Weihmann, D. Martins, and L. Coelho. Force capabilities of kinematically redundant planar parallel manipulators. *13th World Congress in Mechanism and Machine Science*, 2011.

[12] A.G. Ruiz, J.C. Santos, J. Croes, W. Desmet, and M.M. da Silva. On redundancy resolution and energy consumption of kinematically redundant planar parallel manipulators. *Robotica*, 36(6):809–821, 2018. doi: 10.1017/S026357471800005X.

[13] N. Baron, A. Philippides, and N. Rojas. A robust geometric method of singularity avoidance for kinematically redundant planar parallel robot manipulators. *Mechanism and Machine Theory*, 151:103863, 2020. doi: 10.1016/j.mechmachtheory.2020.103863.

[14] R. Boudreau, S. Nokleby, and M. Gallant. Wrench capabilities of a kinematically redundant planar parallel manipulator. *Robotica*, 39(9):1601–1616, 2021. doi: 10.1017/S0263574720001381.

[15] M. Arsenault, R. Boudreau, and S. Nokleby. Determination of the available wrench set of a 3-RPRR kinematically-redundant planar parallel manipulator. *Mechanism and Machine Theory*, 169:104628, 2022. doi: 10.1016/j.mechmachtheory.2021.104628.

[16] A. Ghoul, K. Kara, S. Djeffal, M. Benrabah, and M.L. Hadjili. Artificial neural network for solving the inverse kinematic model of a spatial and planar variable curvature continuum robot. *Archive of Mechanical Engineering*, 69(4):595–613, 2022. doi: 10.24425/ame.2022.141518.

[17] J. Gallardo-Alvarado, K.A. Camarillo-Gomez, and M.A. Garcia-Murillo. A Gough/Stewart-type platform under a combined scheme of actuation. *International Journal of Advanced Manufacturing Technology*, 68:981–991, 2013. doi: 10.1007/s00170-013-4889-x.

[18] K.M. Lynch and F.C. Park. *Modern Robotics: Mechanics, Planning, and Control*. Cambridge University Press, UK, 1st edition, 2017. doi: 10.1017/9781316661239.

[19] J. Gallardo-Alvarado, R. Rodriguez-Castro, and Md. Nazrul Islam. Analytical solution of the forward position analysis of parallel manipulators that generate 3-RS structures. *Advanced Robotics*, 22(2-3):215–234, 2008. doi: 10.1163/156855308X292556.

[20] J. Gallardo-Alvarado and J. Gallardo-Razo. *Mechanisms: Kinematic Analysis and Applications in Robotics*. Academic Press, 2022. doi: 10.1016/C2021-0-02621-3.

[21] R. Von Mises. *Motor Calculus: A New Theoretical Device for Mechanics*. Institute for Mechanics, University of Technology, 1996.

[22] R. Gilmore. *Lie Groups, Lie Algebras, and Some of Their Applications*. Dover Publications, 2006.

[23] J. Gallardo-Alvarado and J.H. Tinajero-Campos. An application of screw theory to the jerk analysis of the PUMA robot. *Archive of Mechanical Engineering*, 72(1):1–30, 2025. doi: 10.24425/ame.2024.153242.

[24] M. Ceccarelli. Screw axis defined by Giulio Mozzi in 1763 and early studies on helicoidal motion. *Mechanism and Machine Theory*, 35(6):761–770, 2000. doi: 10.1016/S0094-114X(99)00046-4.

[25] I. Duleba and I. Karcz-Duleba. A comparison of methods solving repeatable inverse kinematics for robot manipulators. *Archives of Control Sciences*, 28(1):5–18, 2018. doi: 10.24425/119074.

[26] M. Faroni, M. Beschi, L. Molinari Tosatti, and A. Visioli. A predictive approach to redundancy resolution for robot manipulators. *IFAC-PapersOnLine*, 50(1):8975–8980, 2017. 20th IFAC World Congress.

[27] Y. Nakamura. *Advanced Robotics: Redundancy and Optimization*. Addison-Wesley Longman Publishing Co., Inc., USA, 1st edition, 1990.

[28] J. Cavacanti Santos and M. Martins da Silva. Redundancy resolution of kinematically redundant parallel manipulators via differential dynamic programing. *Journal of Mechanisms and Robotics*, 9(4):041016, 2017. doi: 10.1115/1.4036739.

[29] H.L. Vieira, J.V. Fontes, and M. Martins da Silva. Reliable redundancy resolution strategies for kinematically redundant parallel manipulators. *Mechanism and Machine Theory*, 167:104531, 2022. doi: 10.1016/j.mechmachtheory.2021.104531.

[30] Y. Wu, Y. Fu, and S. Wang. Global motion planning and redundancy resolution for large objects manipulation by dual redundant robots with closed kinematics. *Robotica*, 40(4):1125–1150, 2022. doi: 10.1017/S0263574721000941.

[31] W. Kwon, B. Hee Lee, and M. Hwan Choi. Resolving kinematic redundancy of a robot using a quadratically constrained optimization technique. *Robotica*, 17(5):503–511, 1999. doi: 10.1017/S026357479900171X.

[32] T.A. Hess-Coelho, E.L. de Oliveira, R.M.M. Orsino, and F. Malvezzi. Modular modeling methodology applied to kinematically redundant parallel mechanisms. *Mechanism and Machine Theory*, 194:105567, 2024. doi: 10.1016/j.mechmachtheory.2023.105567.

[33] J.J. Craig. *Introduction to Robotics, Global Edition*. Pearson Education, 2021.

[34] J. Flight and C. Gosselin. Kinematically redundant (6+2)-dof HEXA robot for singularity avoidance and workspace augmentation. *Mechanism and Machine Theory*, 195:105615, 2024. doi: 10.1016/j.mechmachtheory.2024.105615.

[35] A. Ginnante, E. Simetti, S. Caro, and F. Leborne. Task priority based design optimization of a kinematic redundant robot. *Mechanism and Machine Theory*, 187:105374, 2023. doi: 10.1016/j.mechmachtheory.2023.105374.

[36] S. Chiaverini, G. Oriolo, and I.D. Walker. Kinematically redundant manipulators. In B. Siciliano and O. Khatib, editors, *Springer Handbook of Robotics*, pages 245–268. Springer, Berlin, Heidelberg, 2008. doi: 10.1007/978-3-540-30301-5_12.